

Deep Reinforcement Learning-Based Automatic Exploration for Navigation in Unknown Environment

Haoran Li, Qichao Zhang, and Dongbin Zhao^{ID}, *Senior Member, IEEE*

Abstract—This paper investigates the automatic exploration problem under the unknown environment, which is the key point of applying the robotic system to some social tasks. The solution to this problem via stacking decision rules is impossible to cover various environments and sensor properties. Learning-based control methods are adaptive for these scenarios. However, these methods are damaged by low learning efficiency and awkward transferability from simulation to reality. In this paper, we construct a general exploration framework via decomposing the exploration process into the decision, planning, and mapping modules, which increases the modularity of the robotic system. Based on this framework, we propose a deep reinforcement learning-based decision algorithm that uses a deep neural network to learn exploration strategy from the partial map. The results show that this proposed algorithm has better learning efficiency and adaptability for unknown environments. In addition, we conduct the experiments on the physical robot, and the results suggest that the learned policy can be well transferred from simulation to the real robot.

Index Terms—Automatic exploration, deep reinforcement learning (DRL), optimal decision, partial observation.

I. INTRODUCTION

AS AN important subproblem of the robot autonomous navigation, automatic exploration means that the robots move ceaselessly to build the entire environmental map in a new environment without any prior knowledge, which is a hot topic in the field of robotics. It has a wide range of scenario applications in practice, such as the search work of rescue robots and the sweeping work of the robot sweepers in the unknown environment. As the robot has to complete the exploration and mapping task in the completely different and unknown environment, the automatic exploration can also reflect the adaptability of the robotic system.

With the spreading attention from various fields, some noticeable works have been yielded, such as the

Manuscript received November 12, 2018; revised April 23, 2019; accepted July 2, 2019. Date of publication August 6, 2019; date of current version June 2, 2020. This work was supported in part by the Beijing Science and Technology Plan under Grant Z181100004618003, in part by the National Natural Science Foundation of China (NSFC) under Grant 61573353, Grant 61803371, Grant 61533017, and Grant 61603268, and in part by Noah's Ark Lab, Huawei Technologies. (*Corresponding author: Dongbin Zhao*)

The authors are with the State Key Laboratory of Management and Control for Complex Systems, Institute of Automation, Chinese Academy of Sciences, Beijing 100190, China, and also with the School of Artificial Intelligence, University of Chinese Academy of Sciences, Beijing 100049, China (e-mail: lihaoran2015@ia.ac.cn; zhangqichao2014@ia.ac.cn; dongbin.zhao@ia.ac.cn).

Color versions of one or more of the figures in this article are available online at <http://ieeexplore.ieee.org>.

Digital Object Identifier 10.1109/TNNLS.2019.2927869

frontier-based [1] and information-based [2] methods. The frontier-based method was to decide the next move of the robot via searching the frontier points that were between free points and unknown points, and the information-based method applied the Shannon entropy to describe the uncertainty of the environmental map and construct the optimization problems, in that way the optimal control variable of the robot can be gained during the automatic exploration process. Unfortunately, in most cases, there is no mathematical optimal solution in the optimization problems constructed by this method. Then, some researchers combined these two methods [3]. This kind of approach employed the Shannon entropy to evaluate the candidate points selected by frontier and then obtained the optimum point in the next move. Furthermore, to make the exploration more efficient and the map more precise, an extra target item was added into the objective function of the optimization problems [4]. However, the computational burden to solve these multi-objective optimization problems will increase rapidly with the increase of the exploration area. In general, the key to the above-mentioned traditional methods is to find the next optimum point according to the current point and the explored map. However, the adaptability is decreased due to the key exploration strategy that is relied heavily on the expert feature of maps, and it is also difficult to design a general terminal mechanism to balance the exploration efficiency and computational burden.

Gradually, the learning-based exploration methods are considered to tackle the above-mentioned problems. Krizhevsky *et al.* [5] adopted deep convolutional neural networks (CNNs) and designed an efficient classification network for large-scale data, which triggered a wave of research on neural networks. CNN has spurred a lot of big breakthroughs in the image recognition area [6]. Meanwhile, the reinforcement learning (RL) has also achieved certain development [7]. Since Mnih *et al.* [7] applied a deep RL (DRL) algorithm and gained better performance than human players in the video game, such as Atari, the algorithm combining with deep learning (DL) and RL became one of the effective tools for complex decision-making problems. Based on Q-learning [8] and the strong feature presentation ability of CNN, deep Q-network (DQN) has shown its tremendous potential in the robot control and game decision making. In the robot control field, the DRL methods in continuous action spaces can establish the mapping from image inputs to the control policy, which is concise [9], [10]. It has many applications in manipulator controlling [11],

intelligent driving [12], and games [13], [14]. In game decision making, the DRL methods in discrete action spaces, such as AlphaGo [15], show the strong search capability within the high-dimensional decision space. Considering these merits of DRL, some researchers attempt to apply it to the exploration and navigation of the intelligent agents in an unknown environment.

Currently, DL or DRL-based methods are mostly adapted in the robotics visual control or navigation tasks, which build the mapping relationship between raw sensor data and control policy. In this way, intelligent agents can move autonomously relying on the sensor data. However, there are two disadvantages to this end-to-end approach. On the one hand, the information provided by mature navigation methods in robotics is ignored, which means that the intelligent agents need to learn how to move and explore effectively from raw data. It definitely increases the training difficulty of intelligent agents. On the other hand, the reality gap between the synthetic and real sensory data imposes the major challenge from simulation to reality. To the best of our knowledge, the reality gap for automatic exploration based on DRL in an unknown environment is not addressed in the existing work.

Motivated by these, we construct an automatic exploration framework based on map building, decision making, and planning modules. This framework makes it easy to combine the fairly complete map building and navigation methods in robotics. Since the visual feature of the built grid map could guide the robot to explore unknown environment efficiently, we propose a DRL-based decision method to select the next target location with the grid map of the partial environment as input. Compared with some existing studies, the main contributions emphasize in two parts.

- 1) In contrast to the end-to-end approach with the raw sensor data as input and control policy as output, our exploration framework combining with traditional navigation approaches can bridge the reality gap from the simulation to physical robots. Meanwhile, the training difficulty is reduced with the proposed framework.
- 2) Compared with the traditional methods [3], [4], we design a value network of DRL and combine the DRL-based decision algorithm with classical robotic methods, which can improve the exploration efficiency and adaptability in an unknown environment.

This paper is organized as follows. Section II describes the related works in robot automatic exploration and the intelligent agent navigation with DRL. Section III presents our definition and analysis of the robot automatic exploration. Then, we give the details of our proposed algorithm and network architecture in Section IV. Furthermore, the simulation experiment and the practicality experiment are displayed, and the comparison among different methods is given. Finally, in Section V, we summarize our work and discuss future work.

II. RELATED WORK

In general, the automatic exploration scheme can be divided into two categories: traditional methods and intelligent methods. The former, which have been attracting considerable

interest since the 1990s, employs expert features of maps for selecting the next goal point. The latter learns the control or strategy directly from the observation based on the learning approaches.

The widely used traditional method for selecting the exploration points was suggested by Yamauchi [1]. This method detected the edges between free space and unexplored space based on the occupancy grid maps and, subsequently, calculated the central point of each edge as the next candidate point. Then, the robot moved to the nearest point by performing the depth-first-search algorithm. However, the safety of the next point is uncertain since the distance between the point and obstacle may be too small. Gonález-Banos *et al.* [3] navigation defined the safety regions and built a Next-Best-View algorithm to decide which region the robot should move to. The simultaneous localization and mapping (SLAM) algorithm and path planning were embedded in this algorithm, where the former was applied to reconstruct the environment and the latter was utilized for generating the actions of the robot.

Another typical traditional method was connected with information theory. Bourgault *et al.* [2] took advantage of the Shannon entropy to evaluate the uncertainty of the robotic positions and the occupancy grid maps and exploited this information metric as the utility of the robot control. The control was derived from a multi-objective problem based on the utility. The utility function of localization was stemmed from the filter-based SLAM algorithms [16]. There is a large volume of existing studies describing the role of the graph-based SLAM algorithm [17]. Different from the filter-based algorithms, the graph-based methods proposed pose graph that applied poses of robots and landmarks as nodes and exploited the control and measurements as edges. Note that new pose caused by the robot movement influenced the covariance matrix of the pose graph. To evaluate the quality of effect from the new pose, Ila *et al.* [18] defined mutual information gain for a new edge in the pose graph. With the rapidly exploring random tree, they searched the paths to explore the unknown environment and used the information gain to evaluate the path entropy; afterward, they choose the one that minimized the map entropy.

Due to the significant recent development in DRL, a number of researchers in intelligent control area attempted to regard the robot exploration as an optimal control problem constructed by the information-based methods and the employ RL to settle the sequence decision problem. Juliá *et al.* [4] modeled the exploration as the partial observation Markov decision process (POMDP) [19] and employed the direct policy search to solve the POMDP. For the great perception ability of DL, it has been widely employed to build powerful methods for learning the mapping from sensor data to the robot control. In 2016, Tai and Liu [20] proposed a perception network with RGB-D image inputs and a control network trained by the DQN. Note that this algorithm only ensures the robot wandering without collision. Bai *et al.* [21] constructed a supervised learning problem to reduce the Shannon entropy of the map. They fed a local pitch of the map into neural networks and predicted which direction the robot should move.

This algorithm often fell into a corner since it only perceived the local environment that was completely explored.

Much of the current studies on intelligent methods pay particular attention to game agents navigation and exploration in a virtual environment. Mirowski *et al.* [22] trained an Asynchronous Advantage Actor-Critic (A3C) agent in a 3-D maze. They embedded long short-term memory (LSTM) into the agent to give it the memory. To improve learning efficiency, they preceded a depth prediction task and a loop-closure detection task. This attempt presented a remarkable performance in this virtual environment. Compared to adding external tasks, Pathak *et al.* [23] proposed an intrinsic curiosity module (ICM). The deep neural network was utilized to encode state features and constructed a world model applied to predict the next step observation in feature space. This model was used to predict the next step observation. The differences between the next step encoder features and the prediction of next step observation features by the world model were employed to drive the agent to move around. Then, Zhelo *et al.* [24] applied this approach in robot navigation. They combined policy entropy and A3C with the calculated robot control.

III. PROBLEM STATEMENT

In order to achieve autonomous navigation, the robot receives sensor data and, simultaneously, builds surroundings map during moving in the unknown environment. To create a more similar map to the actual situation, the robot exploration algorithm is essential. Under traditional navigation frameworks, the robot has to generate the environment map and locate itself. With the development of DL and DRL, there are several end-to-end control methods by DRL over the years. Those methods feed the sensor data and surroundings as the input of the deep neural networks and output the control for the robot.

A momentous advantage of end-to-end methods is concise. However, there is a wide gap to apply the technique to a real robot. The end-to-end learning methods have to conduct massive trial-and-error experiences, so most of the researchers put this learning process in the simulation environment. Consequently, this behavior raises the following three problems.

- 1) The algorithm needs a long time to converge since the robot starts from learning movement to explore the unknown environment.
- 2) Since the real environment is not the exact same with the simulation environment, there is no guarantee that the mapping represented by deep neural network learned under simulation environment has a superior generalization under the real environment.
- 3) The mechanism and sensor errors of the physical robot may cause the intelligent control law to be not applicable to the physical robot.

Based on the above-mentioned issues, we separate the robot exploration into three modules: decision module, mapping module, and planning module. Therefore, we can design the planning algorithms for different robots with the same decision

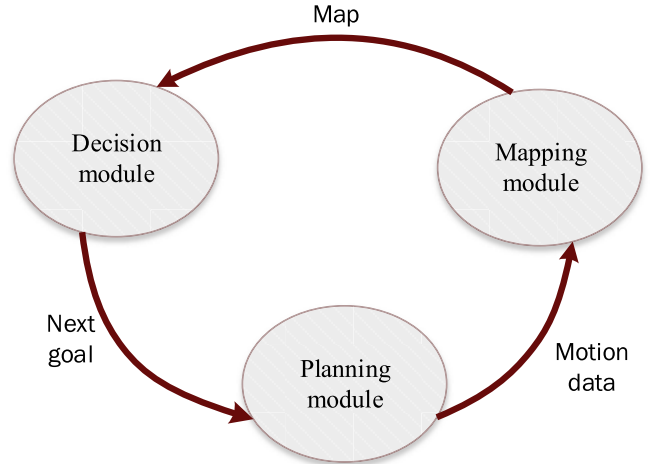


Fig. 1. Relationship between the modules of the exploration framework. Decision module receives data from the mapping module and sends the next goal point to the planning module. Planning module calculates the potential trajectories from the current position to the goal position and sends the control data to the mapping module.

module since each module is independent of each other. The planning algorithms guarantee that robots can move safely without learning in a known environment. With the help of the traditional navigation algorithms, the decision module focuses on the efficient exploration strategy. Fig. 1 describes the relationship between the three modules. In the following, we form each module more general for extensions and unfold each module to explain its function.

A. Decision Module

According to the historical observation, this module chooses the goal point, where the robot should move to. In this paper, the module input is the map of surroundings built by the mapping module. The decision module is modeled as

$$g_t = f_{\text{decision}}(l_{0:t}, m_t) \quad (1)$$

where g_t is the goal point, $l_{0:t}$ are the robot positions from time 0 to t , and m_t is the built surroundings map at time t . There are several efforts focused on figuring out the function f_{decision} ; most methods are based on the frontier methods and with the heuristic search. Those methods are required to establish massive rules for complex environments, which results in heavy dependencies on expertise.

In this paper, we will mainly focus on finding out the more concise and the general function f_{decision} . We propose a DRL-based decision method in Section IV. Compared to the frontier-based method, our method learns the visual feature for exploration automatically. Instead of stacking the rules for exploration, our method learns the feasible strategy from trial and error and covers more complex scenes.

B. Planning Module

This module aims to ascertain the feasible trajectory from the current position to the goal point. The planning module is modeled as

$$\tau_{t:t+T} = f_{\text{planning}}(l_{0:t}, g, m_t) \quad (2)$$

where $\tau_{t:t+T}$ is the planning trajectory for robot control. The widely investigated framework for many planning approaches that implement the planning function includes the global planning method and the local planning method. The aim of the former is to determine the shortest path from the current position to the goal position on the map, and the latter attempts to convert the path to a trajectory and adjust the trajectory based on the real-time sensor data. It should be mentioned that recent studies related to the planning module have shown different frameworks. Those particular methods modeled as deep neural networks take the sensor data and goal point as the input and build the mapping from the input to the control.

Considering that A^* [25] is a simple and efficient search method, we apply A^* as the global planner. The result of A^* search is a path composed of the discrete points, and the path cannot control the robot directly. We employ the timed-elastic-band (TEB) method [26] as the local planner that convert the path into the robot velocity. Compared to the pure tracking, this method can avoid obstacles that are not in the built map (such as moving objects) according to the real-time point cloud from light detection and ranging (LiDAR).

C. Mapping Module

Mapping module processes the sensor data in sequence and produces the robot pose and surroundings map at each timestamp, which is also known as SLAM. The function of the SLAM can be written as

$$m_t, l_t = f_{\text{mapping}}(l_{t-1}, m_{t-1}, u_t, z_t) \quad (3)$$

where u_t and z_t are the control and observation at time t , respectively. The major SLAM methods can be divided into two categories: filter- and graph-based methods. Filter-based methods make use of the Kalman filter or the expand Kalman filter to update the estimation of the robot and landmark (map) pose. The graph-based methods collect the control and the observation to construct a pose graph and take advantage of the nonlinear optimization to estimate the robot pose. Moreover, Parisotto and Salakhutdinov [27] proposed a neural SLAM method that exploited deep neural network fitting the function f_{mapping} .

We utilize a graph-based method named Kart SLAM. It is simple to implement and works well in most scenes. Compared to the filter-based method, the graph-based method can diminish the error and obtain the extract solution consistently. Therefore, more and more papers focus on the graph-based methods recently [17].

In this paper, we place great emphasis on constructing the DRL algorithm for the decision module to implement efficient exploration. Compared with traditional decision methods, the DRL-based decision algorithm can eliminate trivial details of complicated rules. Different from the end-to-end methods, the approaches based on this framework have a higher degree of modularity, and it is more flexible and interpretable.

IV. DRL-BASED DECISION METHOD

A. Objective Function

The objective of the robot exploration is to build an environment map that is most similar to the real environment.

Considering the battery capacity, the robot is designed to select a shorter path to explore the environment. Then, we give the following objective function:

$$c(\hat{m}, x_{t=0:T}) = \min_{u_{t=0:T}} \|m - \hat{m}\|^2 + L(x_{t=0:T}) \quad (4)$$

where \hat{m} is the estimation map, m is the real map, and $L(\cdot)$ is the path length during exploration from $t = 0$ to $t = T$.

However, since the actual map is non-available due to the unknown environment, it is hard to handle the objective function and find the minimum solution. Inspired by the Shannon entropy for the evaluation of the exploration [2], we exploit the occupancy grid map to represent the environment. Note that $p(m_{i,j})$ is the occupied probability of the cross grid of i th column and j th row. Each grid has three possible states: unknown, free, and occupied. In addition, the entropy of the map is

$$H(m) = - \sum_i \sum_j p(m_{i,j}) \log p(m_{i,j}). \quad (5)$$

This objective function evaluates the uncertainty of the built map.

B. Deep Reinforcement Learning

We take exploration as a sequence decision-making task. A Markov decision process defined as a tuple $\langle S, A, T, R, \gamma \rangle$ is a framework for decision making. S denotes a finite set of states. A is the set of the actions that the agent can take. $T(s'|s, a)$ is the transform distribution over the next state s' , given the agent took the action a with the state s . $R(s, a)$ is the reward the agent receives after taking action a in state s . γ is the discount factor. The goal of the agent is to maximize the expectation of the long-term cumulative reward $V(s)$

$$V(s) = \max \sum_{t=1}^T E_{(s_t, a_t) \sim p_\theta(s_t, a_t)} [r(s_t, a_t)]. \quad (6)$$

RL is an intelligent method for the robot control [28]. Q-learning is a popular method to learn an optimal policy from the samples generated from interactions with the environment. The key to Q-learning is calculating the Q value function that evaluates the action took in the state. and the optimal Q value obeys the Bellman optimal equation as follows:

$$Q^*(s, a) = E_{s'}[r + \gamma \max_{a'} Q^*(s', a')|s, a]. \quad (7)$$

Since this optimization problem is nonlinear, it is difficult to obtain the analytic solution. The common iterative method for this problem is the value iteration as follows:

$$\begin{aligned} Q(S_t, A_t) \leftarrow & Q(S_t, A_t) + \alpha[R_{t+1} + \gamma \max_{a' \in A} Q(S_{t+1}, a')] \\ & - Q(S_t, A_t)]. \end{aligned} \quad (8)$$

Note that recent advances in DL have facilitated the investigation of feature extraction. Mnih *et al.* [7] took a deep neural network as a function approximation for the Q value function and trained the networks by minimizing the mean squared error (mse)

$$L^{\text{DQN}} = E[(R_{t+1} + \max_{a' \in A} Q(S_{t+1}, a'; \theta^-) - Q(S_t, A_t; \theta))^2] \quad (9)$$

where $(S_t, A_t, R_{t+1}, S_{t+1})$ are sampled from the experience replay buffer collected by the agent. This DQN algorithm achieved a huge success in many games, such as Go and Atari.

Recently, many researchers introduced the DQN algorithm for robot navigation. Most of them apply the original sensor data as the algorithm inputs, such as point clouds of LiDAR [29] and images [30]–[33]. With the powerful representation of the deep neural networks, these methods can extract key features without expert experiences. Nevertheless, compared to the empirical features, the original sensor data have a higher dimension, which increases state space sharply. From this perspective, the agent has to take massive trial and error to cover all the potential state-action combination, which takes a long time. In view of the safety and lifetime of the real robots, it is impossible to take the extensive trials in the real environment. Hence, most researches trained the agent in a simulated environment. However, there are two common problems in transferring the virtual agent into a real agent. First, since the error functions of the sensors are different between virtual and real environment, it is hard to guarantee the good generalization of the DRL algorithm from virtual to real. Second, due to the mechanical error, it is uncertain that the real robots will have an excellent performance with the control law learned in a virtual environment.

As discussed earlier, we introduce the hierarchy decision framework in Section III. We separate the decision module from the planning module. The decision module provides the next goal point, and the planning module plans the path from the current position to the goal point. In this way, the control policy derived from the traditional optimal control has a good match with the real robot.

In this section, we aim to design a novel DRL algorithm for the decision module. The inputs of the decision module are map, current, and historical robot positions obtained from the mapping module. We obtain the optimal decision sequence

$$\begin{aligned} x_{t=0:T}^* &= \arg \min H(m_T) + L(x_{t=0:T}) \\ &= \arg \min H(m_T) - H(m_0) + L(x_{t=0:T}) \\ &= \arg \min \sum_{t=1}^T [H(m_t) - H(m_{t-1})] + \sum_{t=1}^T L(x_{t-1}, x_t) \\ &= \arg \max \sum_{t=1}^T [H(m_{t-1}) - H(m_t) - L(x_{t-1}, x_t)]. \quad (10) \end{aligned}$$

Therefore, we can define the reward function for exploration as follows:

$$r_t = \alpha(H(m_{t-1}) - H(m_t) - L(x_{t-1}, x_t)) \quad (11)$$

where α is coefficient to make the training process more stable.

In view of the safety, we attach the heuristic reward function, such as

$$r_t = \begin{cases} -1, & \text{if the next point is in unknown space} \\ -1, & \text{if the next point is too close to the obstacle.} \end{cases}$$

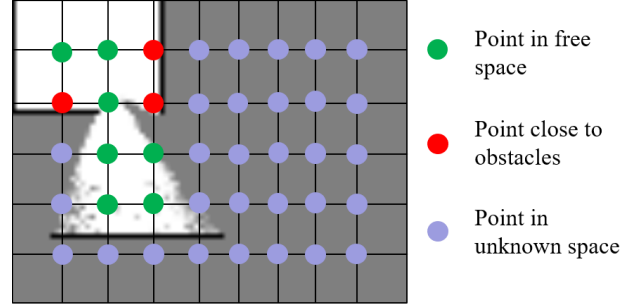


Fig. 2. Action space based on the occupancy grid map. In the grid map, the white and gray areas are the free and unknown spaces, respectively. The black edges are the occupied grids that are the contours of the obstacle. The points are the action positions that are sampled regularly from the grid map. The green points are safe actions, and others are dangerous.

To stop the exploration in time, we introduce the terminal action and define the reward for this action

$$r_t = \begin{cases} 1 & \text{if the ratio of explored region in map } \rho > 0.85 \\ -1 & \text{otherwise.} \end{cases}$$

Remark 1: The target of automatic exploration is to build the map of the unknown environment based on the navigation and mapping technique. Note that the logic of reward signal is designed based on safety and efficiency. As the robot cannot confirm the dangerous status of the unknown space that may be the obstacle, wall, and so on. Therefore, a penalty signal is given to encourage the robot to choose the next goal point in the free space. Besides, we hope the distance from the goal point to the obstacles will be larger than the robot geometrical radius in consideration of collision avoidance. Combined with the designed efficient exploration logic, the robot can find out the safety and efficient policy in an unknown environment. It should be mentioned that the ratio ρ is a hyperparameter to balance the explored region rate and the explored efficiency. Here, we choose it as 0.85 based on experiments.

C. Action Space and Network Architecture

The action of exploration is selecting a point from the built map. Since we utilize the occupancy grid map, the action space is discrete. To simplify the problem and reduce the searching space, we exploit the rasterized sampling on the grid map, and the action space is composed of these sampling points. Fig. 2 describes the occupancy grid map and the action space for the proposed algorithm.

Since the points in action space are obtained from regularly sampling, we can design a CNN to estimate the value of each point in the map. The designed network architecture is shown in Fig. 3. The lower layers are encoder layers, where the output dimension is the same as the action space.

To estimate the Q values, we construct a network named fully convolutional Q-network (FCQN) based on the two convolutional branches after encoder layers. The one applies convolution to calculate score map that has the same size with encoder feature maps. Each element of the score map represents the advantage function of the corresponding point

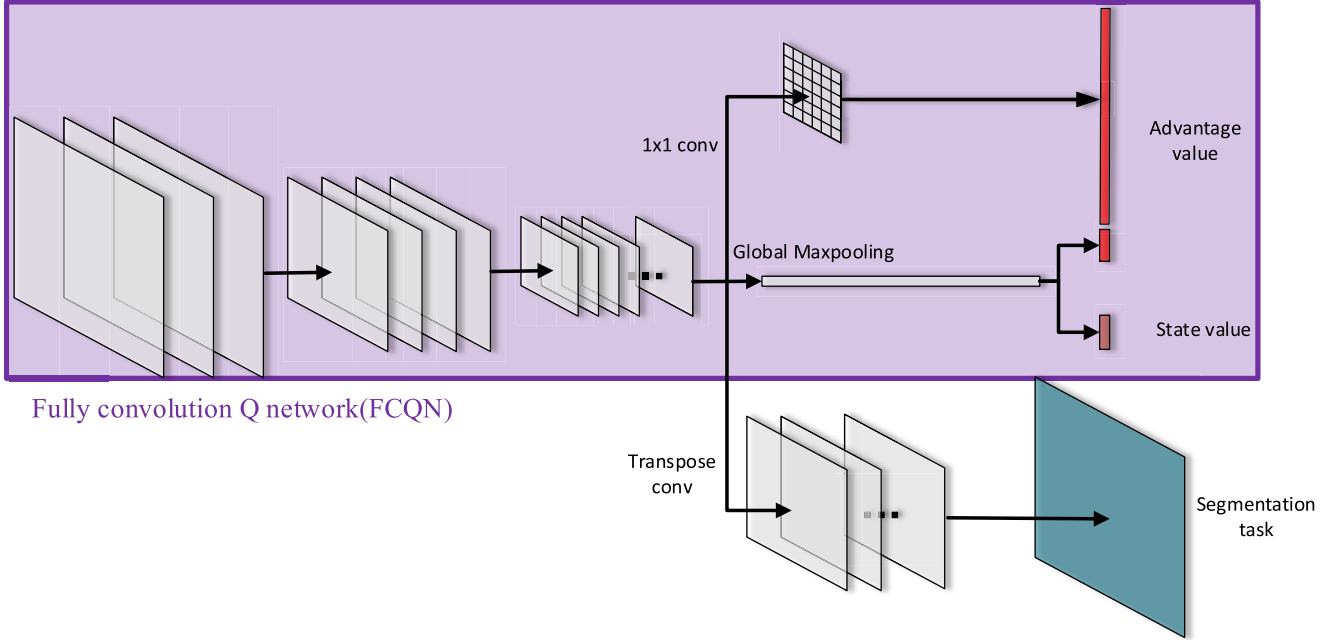


Fig. 3. FCQN with an auxiliary task. The lower layers of this network are convolutional as in the original DQNs.

in action space. The other exploits the max-pooling operation to collect the feature vector of the whole map. Subsequently, the fully connection layer estimates the advantage value of the terminal action and the state value. The Q value of each point action is derived from [34]

$$Q(s, a; \alpha, \beta) = V(s; \beta) + \left(A(s, a; \alpha) - \frac{1}{|A|} \sum_{a'} A(s, a'; \beta) \right). \quad (12)$$

The terminal action Q value is

$$Q(s, a; \beta) = V(s; \beta) + \left(A(s, a; \beta) - \frac{1}{|A|} \sum_{a'} A(s, a'; \beta) \right). \quad (13)$$

Compared with the original DQNs architecture, our network makes several significant improvements. One the one hand, the FCQN is more accessible to train and has less overfitting risk due to the fewer parameters. The original DQNs employ fully connected layer after flattening feature maps and introduce massive trainable parameters. By contrast, the FCQN only has several convolutional kernel parameters. The fully connected layer in the original DQNs needs the inputs to have the same dimension, which restricts its adaptability for the environment with various sizes. On the other hand, since the fully convolutional network accepts different size inputs, the FCQN has better adaptability for the changeable map size. Those properties make our network more convenient to train in a new environment continuously.

D. Auxiliary Task

Compared with the empirical features, putting the map image as the input of DRL increases the search space rapidly.

The agent needs more time to analyze every possible state-action combination, which increased difficulties in the training process.

Some researchers proposed auxiliary tasks by enhancing prior knowledge to improve training efficiency. Mirowski *et al.* [22] implemented depth prediction and loop-closure prediction as the auxiliary task to improve the performance and training efficiency of the DRL algorithms. Lei and Liu [20] trained the deep convolutional network with classification task and then exploited this network to extract the features for the RL. The feature input drastically reduces the state dimension and exploration time instead of the original image input. Unfortunately, these features are usually not the task-oriented, and there is no guarantee for the quality of the features.

Considering the crucial roles of the map edge in navigation and exploration, we present the edge segmentation as the auxiliary task for FCQN. Note that the edges composed of two elements. One is the contour of obstacles, which is essential for avoiding the collision during navigation. The other is the boundary between free space and unknown space. This boundary is named frontier employed to produce the candidate points.

The third branch for segmentation appended in the network architecture, as shown in Fig. 3. We call the whole network with segmentation branch as FCQN with an auxiliary task (AFCQN). We apply the decoder block that consists of twice deconvolution after lower feature maps. The output of this branch has the same dimension as the input map. The loss function for this branch is

$$L_s = - \sum_p \sum_{c=1}^M y_{o,c} \log p_{o,c} \quad (14)$$

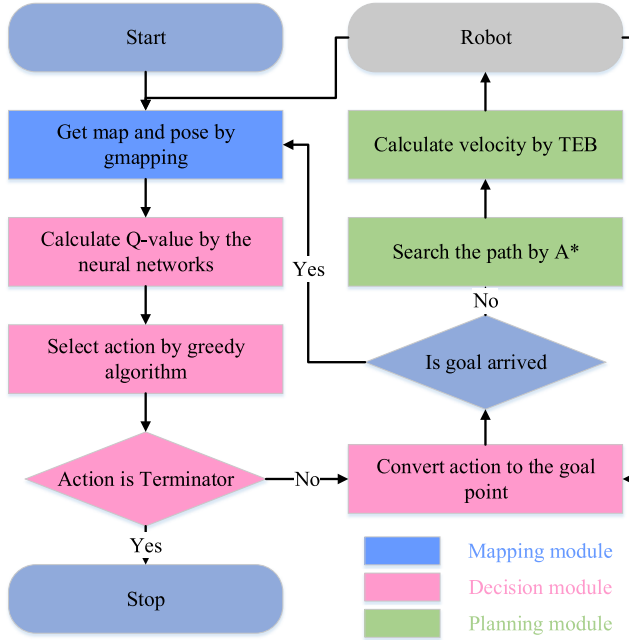


Fig. 4. Diagram of the automatic exploration system.

where p represents the pixel in the map and M is the set of the possible classes. In this case, M includes three types, such as the contours of the obstacle, frontiers, and others. $y_{o,c}$ is the binary indicator if the class label c is the correct classification for observation o , and $p_{o,c}$ means that the predicted probability observation o is of the class c .

Therefore, the lower convolutional layers update the parameters by two-part back-propagation error

$$\Delta w = -\epsilon \left(\frac{\partial L^{\text{DQN}}}{\partial w} - \lambda \frac{\partial L_s}{\partial w} \right) \quad (15)$$

where ϵ and λ are the learning rate and the balance parameter for the segmentation task, respectively, and w is the parameter of the lower convolutional layers. These analytical procedures and the results are described in Section VI.

V. WHOLE SYSTEM

The workflow of the whole system is shown in Fig. 4. The robot collects the odometry data and the point cloud data by scanning the environment and sends the data to the mapping module. In this paper, we apply the gmapping method as the mapping module that builds the map and obtains the pose in the built map. Based on the results of mapping module, we propose novel DRL-based decision algorithms (FCQN and AFCQN, where we use AFCQN as the example) that utilize the built mapping and the localization as the input and give the next goal point. As the global planner, A^* algorithm receives the goal point from the decision module and the built map from the mapping module. It searches the feasible path that is composed of discrete points. The local planner translates the path to the velocity and sends to the robot. The robot moves around in the environment, receives the new sensor data, and builds a new map. Then, it begins the new process loop.

VI. EXPERIMENTS

In this section, we conduct experiments in the simulated world and the physical world to compare the performance of different algorithms. In our exploration framework, we present the DRL-based method as the decision algorithms. For the mapping module, we make use of the graph-based methods, where the front end is based on the scan matching method [35] and the back end is based on the graph optimization implemented by the g2o package [36]. The planning module is composed of the A^* search methods as the global planner and TEB as the local planner. First, we compare the different networks, including the original DQN and the proposed FCQN and AFCQN with same state space and action space. Then, we conduct experiments to find the similarity and difference between AFCQN and the frontier-based method. Finally, we deploy the algorithms on the real robot.

A. Evaluation Metrics

To compare the performance of different algorithms, we define the explored region rate, average path length, and exploration efficiency.

Explored region rate embodies the completeness of the map built during exploration. It is defined as

$$\text{Explored region rate} = \frac{\text{Number of explored free cells}}{\text{Number of free cells in the real map}}. \quad (16)$$

With the high-explored region, we hope the agent move efficiently. Therefore, the average path length and exploration efficiency are introduced

$$\text{Average path length} = \frac{\sum_i L_{\tau_i}}{\text{Number of episodes}} \quad (17)$$

$$\text{Exploration efficiency} = \frac{\sum_i (H(T) - H(0))_i}{\sum_i L_{\tau_i}} \quad (18)$$

where L_{τ_i} is the path length of the trajectory τ_i during the i th episode.

In general, a larger explored region rate leads to a longer path. Thus, the larger explored region rate and the shorter path are inconsistent. Exploration efficiency represents the entropy reduced per unit length, and it is a compromise metric for exploration.

B. Simulation Setup

We construct the simulation platform based on the Stage package [37] of robot operation system (ROS) for agent training. We create a virtual map for algorithms training and design the maps with different layouts and sizes for testing. Fig. 5 and Table I show the details of the maps. The kinematic model of the agent is omnidirectional, which can go left or right without rotation.

C. Training Analysis

We conduct the training process on the training map. The inputs of the algorithms are the combined images, including

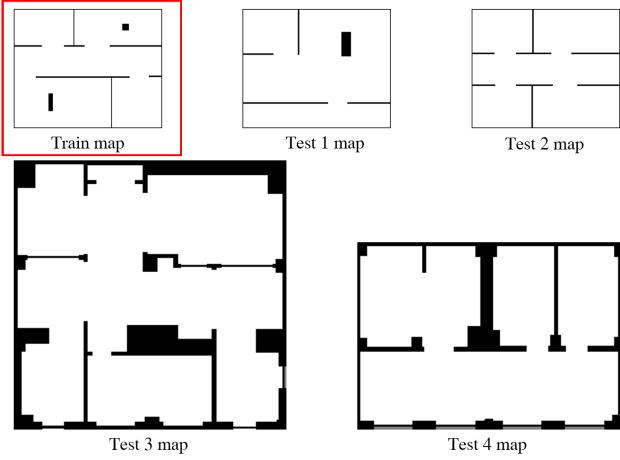


Fig. 5. Maps for training and test.

TABLE I
DETAILS OF THE TRAINING AND TEST MAPS

Map name	Resolution	Real size(meter)
Training map	161×201	5×8
Test map 1	161×201	5×8
Test map 2	161×201	5×8
Test map 3	273×277	13.65×13.85
Test map 4	190×267	9.5×13.35

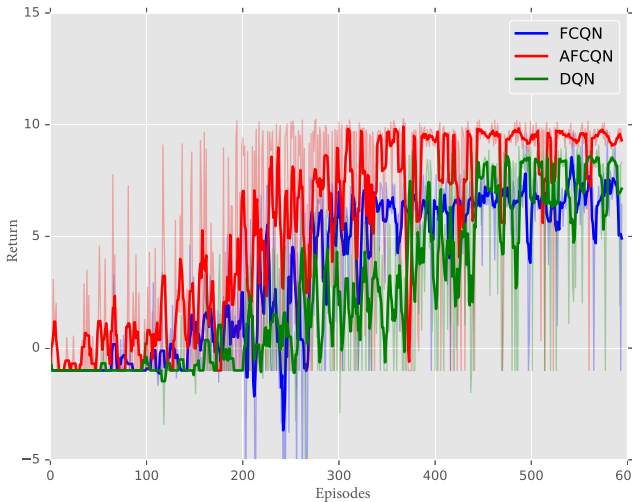


Fig. 6. Return during training.

the grid map, the current position map, and the last position map. The position map draws the robot position on the blank map that has the same size as the built map.

Fig. 6 shows the training processes. The returns grow during the training episodes and converging to the stable value. We can see that FCQN learns faster than DQN, but the final return is slightly smaller than DQN. The possible reason for this appearance is that DQN has more parameters than FCQN and better ability to remember the complex decision sequences. Since AFCQN uses more information to find out the optimal parameters, AFCQN has a better performance in convergence speed and final return.

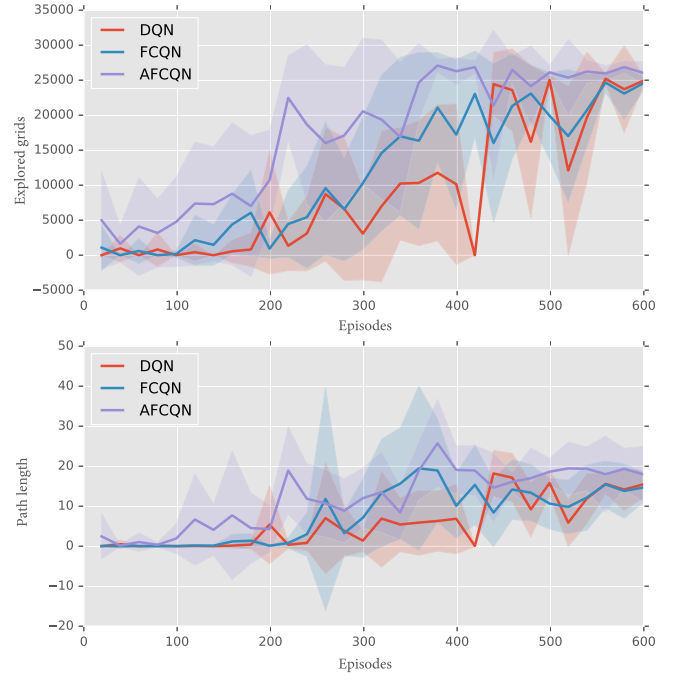


Fig. 7. Explored grids and path length during training. The bold curves are average values over episodes. The shadow of each curve is corresponding to the variance.

TABLE II
RESULTS ON THE TRAINING MAP

Methods	Explored region rate	Path length	Explored efficiency
AFCQN	mean	0.91	24.39
	std	0.0028	311.0449
FCQN	mean	0.85	16.46
	std	0.0414	2.8107
DQN	mean	0.84	1108.51
	std	0.2190	190.8171

Fig. 7 describes the number of explored grids and the path length during the training episodes. From the picture, we find out the edge segmentation task speeds up the exploration. AFCQN learns the safe strategy for movements and increases the path length quickly. However, the segmentation task also brings redundant movements that do not increase the new free cells. With the iteration of Q values, the algorithm crops the redundant movements and achieves the better return.

To compare the trained algorithms in the training map, we conduct 50 trials by selecting the initial points randomly from free space. Results are shown in Table II. All algorithms finish the exploration completely on the training map, and AFCQN has highest explored region rate, while FCQN has the highest exploration efficiency. The reason for high-explored efficiency for FCQN is selecting the terminal action in time, which avoids the redundant movement. AFCQN has more attention on the completeness of the built map, which leads to the longer path. For most trials, DQN has a higher explored region rate than FCQN, but it fails in some cases. Fig. 8 shows the comprehensive performance. The curve means the proportion of the episodes that achieve the specified explored

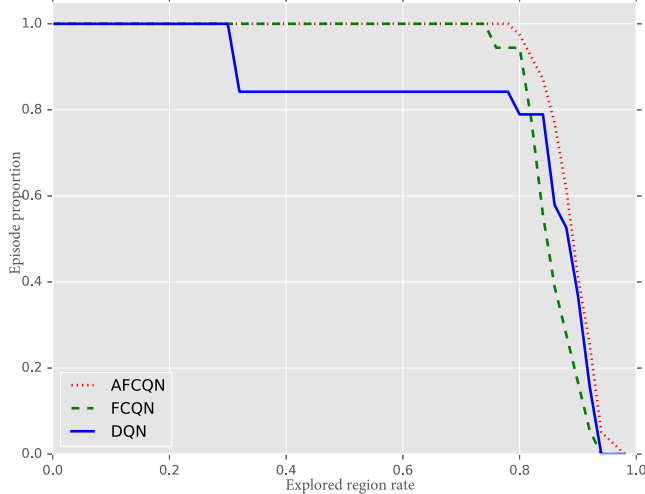


Fig. 8. Episode proportion in trials goes with explored rate, while the exploration path length is shorter than 25 m.

region rate within 25 m. According to Fig. 8, we see that AFCQN has a better performance than others, and FCQN has a stable performance, where its explored region rate distributes around 0.8. Except for the failed cases, the explored region rate of DQN distributes around 0.9.

D. Generalization Analysis

In order to analyze the generalization of the algorithms, we design the test maps different from the train map. Considering the constraint of the stand DQN caused by the fully connected layers, we design two maps (test map 1 and test map 2) as shown in Fig. 5 with the same size but different layouts with the train map. Our algorithms based on the fully convolutional layer adapt well with variant map sizes. In addition, we design the two maps (test map 3 and test map 4) with different sizes with the train map. We test our algorithms on these maps, and the results are shown in Fig. 9.

According to Fig. 9, all algorithms have good generalization on the test maps that have different layouts from the train map. AFCQN has the highest explored region rate in test map 1, and FCQN follows. AFCQN and FCQN have the same explored region rate in test map 2, while FCQN has a less standard deviation. In addition, FCQN has a shorter path length. FCQN has a better performance than DQN. Compared to results in the training map, AFCQN has a higher explored region rate and less explored region rate standard deviation than others in test maps.

Since the fully connected layers of DQN restrict its output dimension, DQN has poor adaptability for different size maps. Note that AFCQN and FCQN make use of fully convolutional layers instead of fully connected layers. They can address different size maps and adjust the output dimension adaptively with keeping a downsampling rate for generating action space. In this part, we compare the difference between AFCQN and FCQN. Although the layout and size are different from the train map, our proposed algorithms work well in new environments. AFCQN has a higher explored region rate.

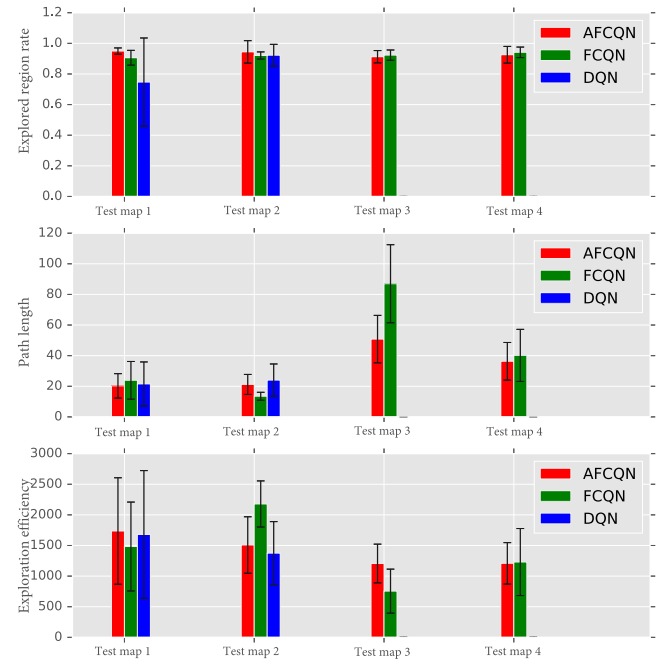


Fig. 9. Statistic results of different algorithms in four test maps. Histogram means the average value for different metrics, and the error bar is the standard deviation.

However, FCQN has a higher exploration efficiency. The changes in layout and scale increase the standard deviation of the explored region rate.

From the above-mentioned two groups of experiments, AFCQN and FCQN are better than DQN in all maps. The layout of the map has an influence on the algorithms. Comparing the test map 1 and test map 2, we can find the common feature between the training map and test map 2, that is, they both have many rooms and “doors.” The layouts of the test maps 1 and 3 are relatively spacious. With this special feature, FCQN has a better performance in exploration efficiency. The reason for this result is that FCQN can end the exploration in time and has shorter exploration path. Note that we add the edge segmentation as the auxiliary task, and AFCQN focuses on the completeness of the built map (since AFCQN has higher explored region rate) and has longer exploration path, which leads to lower exploration efficiency. In spacious environments, such as test map 1 and test map 3, the exploration strategy is simple than in crowded environments, such as test map 2 and training map. This means that it is easier to complete exploration. AFCQN can detect the completeness of the built map and end the process in time. FCQN needs more step to confirm the finish. These results show that AFCQN has better ability to detect the completeness of the built map.

E. Relationship to Frontier-Based Methods

Since AFCQN takes the edge segmentation as the auxiliary task, we further analyze how this task affects the decision of AFCQN. In the frontier-based methods, the frontiers that are the boundaries between free space and unknown space are the

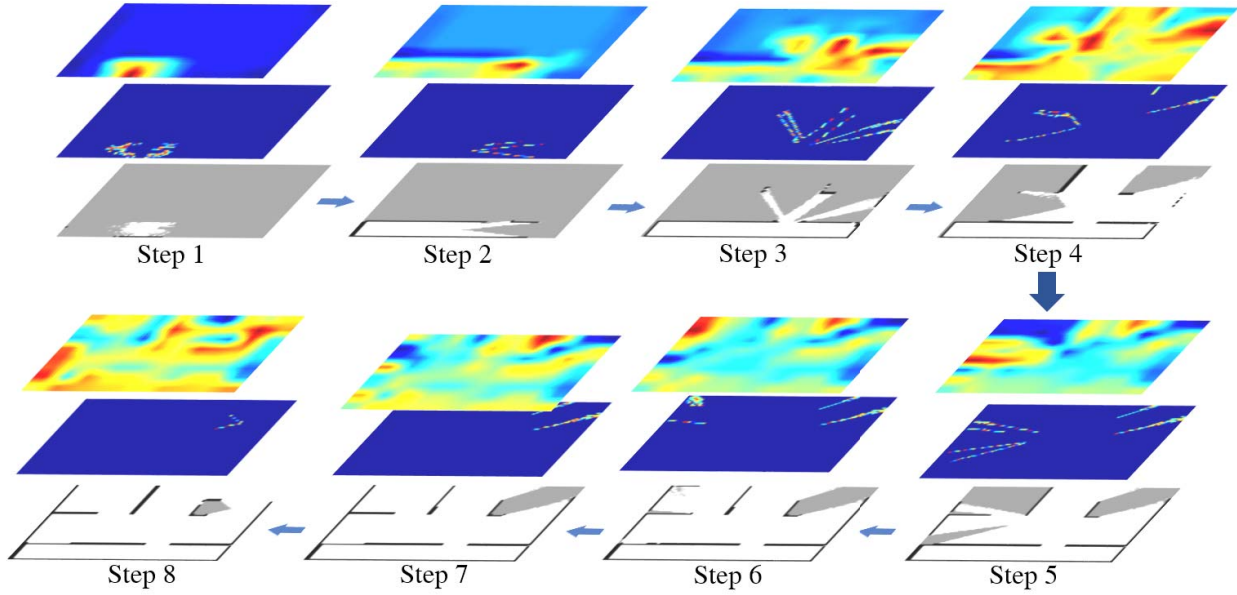


Fig. 10. Decision process of AFCQN during exploration. The whole process composed of eight steps. Each step has three layers including built occupancy grid map (bottom), frontier (middle), and Q value map (top). After the eighth step, AFCQN selects the terminal action and stops the exploration.

decision candidates, so we compare the decision process of AFCQN to the frontier-based methods. Fig. 10 describes the process.

In the early decision stage, the valuable decision positions distribute around the frontiers. With the expanding of the map, the frontiers speed out. AFCQN learns intuition for maximizing the increasing free cells. In step 5, the algorithm selects the center of frontiers in the left part of the map. It is more efficient than selecting a center of any frontier. In step 6, there are two frontiers on the map. The top right frontier is the candidate, which increases more free grids. The top left frontier will increase a few free grids but closer to the current position. It can be seen that AFCQN selects the top left point first and the top right point second. This strategy is better than selecting the top right first for considering the completeness and the whole path length. After step 8, AFCQN selects the terminal action to stop the exploration.

We also compare AFCQN with the frontier-based method. Fig. 11 shows the results on the four test maps. The frontier-based method achieves a higher explored region rate. Since the decision point of this method is selected from frontier centers, it explores the environment continually until there are no reachable points. In other words, it usually has a long path. Although AFCQN is inspired by the built map edges, it estimates the status of the whole maps in order to select the terminal action in time. Therefore, AFCQN has higher exploration efficiency in the first three test maps.

Fig. 12 presents the stability of the algorithms. With constraints of the distance, the frontier-based method is better than AFCQN. However, the frontier-based method also faces with some special cases that make exploration fail. We explain one case in Fig. 13. LiDAR receives the point cloud and renders to grid map. The frontier-based method detects the frontiers shown as red grids and calculates the center represented by

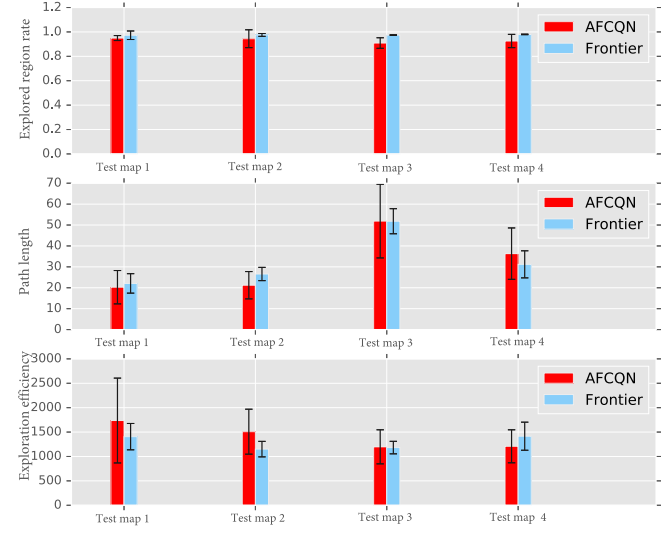


Fig. 11. Statistic results of AFCQN and frontier-based method in four test maps. Histogram means the average value for different metrics, and the error bar is the standard deviation.

a green ball. Unfortunately, the robot is standing at this center point, and then, it stops the exploration. Since the inputs of AFCQN include the robot current position and last decision position, this case never happens during the conducting AFCQN method.

F. Physical World Experiments

Since our algorithm output is the decision point instead of the robot control, it is easier to transfer to the physical robot. We employ the DJI Robomaster robot platform shown in Fig. 14. The major components include the gimbal and the chassis. The chassis equips with the Mecanum wheel for

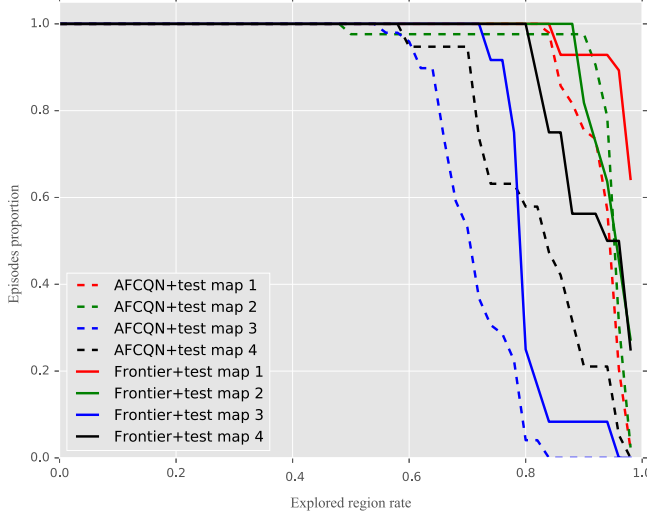


Fig. 12. Episodic proportion in trials goes with explored rate.

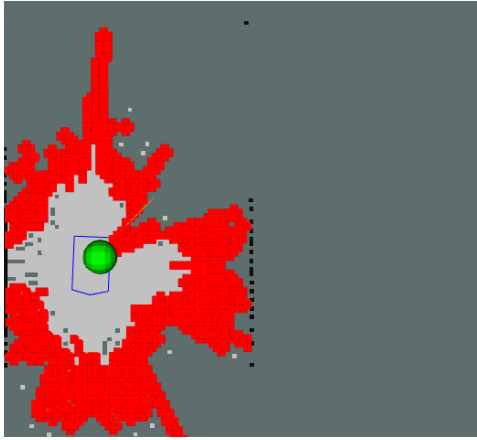


Fig. 13. Frontier-based methods fail case. The blue polygon is the base of the robot. The red grids are frontiers. The green ball is the center of the frontiers. In this case, since the robot position and frontiers center overlap, the exploration stops.

omnidirectional movements. We fixed an RPLiDAR that has similar properties with simulated LiDAR on the chassis for mapping. Then, we test our algorithm with the platform in the real environment.

Here, we show the results of the physical world experiment to the simulated world. The simulated map and built real-world map are shown in Fig. 15. Due to the difference in sensor errors and environments, the observations of their experiments are different. Table III shows the comparing results. The Frontier-based methods have the highest explored region rate in both the physical world and the simulated world. However, our proposed method AFCQN has best-explored efficiency since our method monitors the completeness of the built map and stop the exploration in time. It is obvious that the distinction between the two observations impacts the explored region rate. DQN is sensitive to inputs and fails to explore the physical world for several times. For other methods, the variances of the explored region rate are the same. Those differences have no effect on exploration path length.

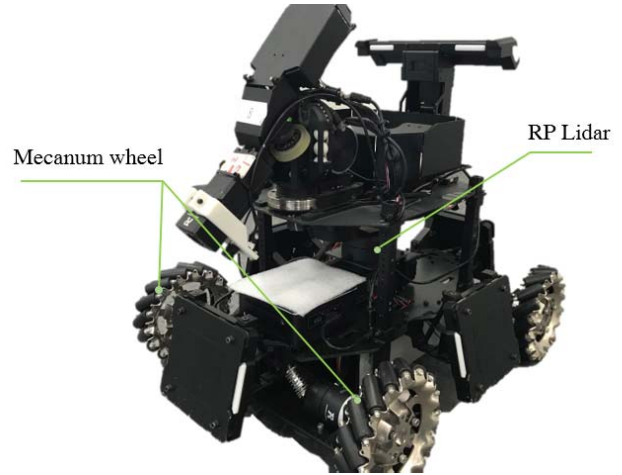


Fig. 14. Hardware of the DJI Robomaster platform.

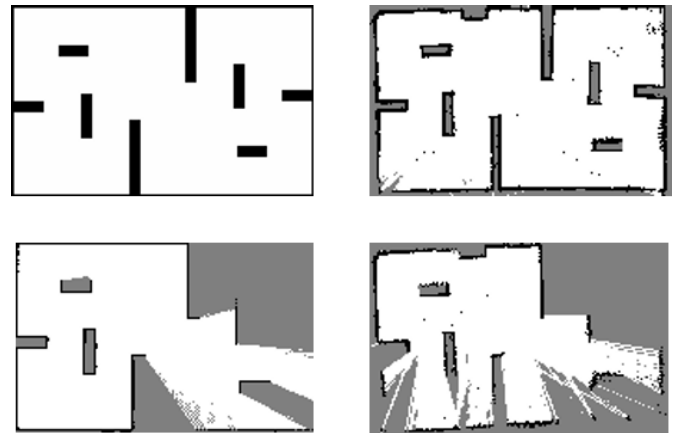


Fig. 15. Simulation map (top left) and the real built map (top right). The bottom left image is the observation (built map) coming from the simulation environment and the bottom right image comes from the real-world environment.

TABLE III
RESULTS OF THE REAL-WORLD AND SIMULATION EXPERIMENTS

Environment	Methods		Explored region rate	Path length	Explored efficiency
Real	AFCQN	mean	0.84	14.76	863.82
	AFCQN	std	0.0344	3.9634	227.0628
	FCQNN	mean	0.78	16.18	796.37
	FCQNN	std	0.0543	4.2317	214.7032
Sim	DQN	mean	0.54	6.87	410.21
	DQN	std	0.4173	5.8931	340.1092
	Frontier	mean	0.91	19.23	840.79
	Frontier	std	0.0134	2.0172	167.3728
Sim	AFCQN	mean	0.92	15.78	986.95
	AFCQN	std	0.0325	6.2216	347.7612
	FCQNN	mean	0.87	16.58	925.74
	FCQNN	std	0.0473	8.3158	314.8210
Sim	DQN	mean	0.81	17.23	806.94
	DQN	std	0.1917	9.0315	425.1479
	Frontier	mean	0.95	17.19	962.34
	Frontier	std	0.0127	2.1475	185.6325

The variance of the path length is decided by the local planner, and we have different local planner parameters for simulation and real experiments in order to adapt different kinematic models. To explain the AFCQN behavior, the exploration trajectories of AFCQN in the trails are shown in Fig. 16. The most trajectories of the real experiments overlap with those

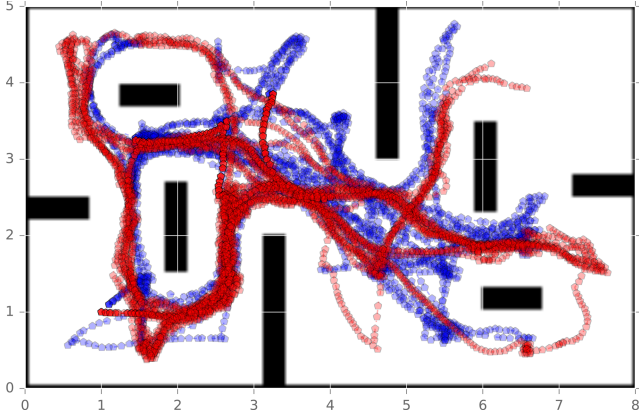


Fig. 16. Exploration trajectories of AFCQN in trials. The red trajectories come from simulation experiments, while the blue trajectories come from real experiments.

of the simulation experiments, and the results imply that the decision processes of the two experiments are similar.

VII. CONCLUSION

In this paper, we construct a novel framework for robot exploration based on the mapping, decision, and planning modules, and we declare the general model for each module. Under this framework, each module is mutual independent and can be implemented via various methods.

The key contribution of this paper is proposing a decision algorithm based on DRL that takes the partial map as the input. In order to improve the training efficiency and generalization performance, we attach the edge segmentation task to train the feature-extracting networks auxiliary.

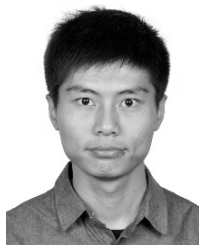
Since the proposed framework is combined with the existing navigation algorithms, the algorithms based on the framework learn faster than the end-to-end methods [20], [22] that undergo thousands of episodes. The experiments show that AFCQN has better generalization performance in different maps compared to the end-to-end methods and stand DQN. Compared to the frontier-based method, AFCQN can avoid failed case and make use of properties of the sensor to explore the environment more efficiently, which makes the decision module look more intelligent. The experiments in the physical world show that our algorithm is easy to transfer from the simulator to the physical world with a tolerable performance.

However, there are some further studies. Since the gridding map is used to generate discrete actions, the final decision sequence based on the discrete action space is suboptimal. The Hilbert occupancy map [38] is a potential substitute, which is used to find out the optimal exploration path in a given map. How to combine this map and policy gradient method is a valuable topic. The deep recurrent neural networks can be adapted to improve the online learning performance [39], and it can be introduced to this task to augment the memory of the algorithm. In addition, how to embed the available auxiliary information and domain knowledge into the DRL method is also a very meaningful research topic for automatic exploration.

REFERENCES

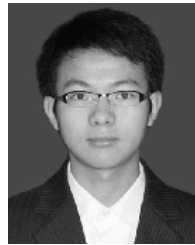
- [1] B. Yamauchi, "A frontier-based approach for autonomous exploration," in *Proc. IEEE Int. Symp. Comput. Intell. Robot. Automat. (CIRA)*, Jul. 1997, pp. 146–151.
- [2] F. Bourgault, A. A. Makarenko, S. B. Williams, B. Grocholsky, and H. F. Durrant-Whyte, "Information based adaptive robotic exploration," in *Proc. IEEE Int. Conf. Intell. Robots Syst. (IROS)*, vol. 1, Sep./Oct. 2002, pp. 540–545.
- [3] H. H. González-Baños and J.-C. Latombe, "Navigation strategies for exploring indoor environments," *Int. J. Robot. Res.*, vol. 21, nos. 10–11, pp. 829–848, Oct. 2002.
- [4] M. Juliá, A. Gil, and O. Reinoso, "A comparison of path planning strategies for autonomous exploration and mapping of unknown environments," *Auton. Robots*, vol. 33, no. 4, pp. 427–444, Nov. 2012.
- [5] A. Krizhevsky, I. Sutskever, and G. E. Hinton, "Imagenet classification with deep convolutional neural networks," in *Proc. Adv. Neural Inf. Process. Syst. (NIPS)*, Dec. 2012, pp. 1097–1105.
- [6] Y. LeCun, Y. Bengio, and G. Hinton, "Deep learning," *Nature*, vol. 521, no. 7553, pp. 436–444, May 2015.
- [7] V. Mnih *et al.*, "Human-level control through deep reinforcement learning," *Nature*, vol. 518, no. 7540, pp. 529–533, Feb. 2015.
- [8] R. S. Sutton and A. G. Barto, *Reinforcement Learning: An Introduction*, vol. 1. Cambridge, MA, USA: MIT Press, 1998.
- [9] T. P. Lillicrap *et al.*, "Continuous control with deep reinforcement learning," 2015, *arXiv:1509.02971*. [Online]. Available: <https://arxiv.org/abs/1509.02971>
- [10] B. Kiumarsi, K. G. Vamvoudakis, H. Modares, and F. L. Lewis, "Optimal and autonomous control using reinforcement learning: A survey," *IEEE Trans. Neural Netw. Learn. Syst.*, vol. 29, no. 6, pp. 2042–2062, Jun. 2018.
- [11] Y. Zhu, D. Zhao, H. He, and J. Ji, "Event-triggered optimal control for partially unknown constrained-input systems via adaptive dynamic programming," *IEEE Trans. Ind. Electron.*, vol. 64, no. 5, pp. 4101–4109, May 2017.
- [12] D. Zhao, Z. Xia, and Q. Zhang, "Model-free optimal control based intelligent cruise control with hardware-in-the-loop demonstration [research frontier]," *IEEE Comput. Intell. Mag.*, vol. 12, no. 2, pp. 56–69, May 2017.
- [13] Y. Zhu, D. Zhao, and X. Li, "Iterative adaptive dynamic programming for solving unknown nonlinear zero-sum game based on Online data," *IEEE Trans. Neural Netw. Learn. Syst.*, vol. 28, no. 3, pp. 714–725, Mar. 2017.
- [14] Q. Zhang, D. Zhao, D. Wang, and Y. Zhu, "Experience replay for optimal control of nonzero-sum game systems with unknown dynamics," *IEEE Trans. Cybern.*, vol. 46, no. 3, pp. 854–865, Mar. 2016.
- [15] D. Silver *et al.*, "Mastering the game of Go with deep neural networks and tree search," *Nature*, vol. 529, no. 7587, pp. 484–489, Jan. 2016.
- [16] A. Stentz, D. Fox, and M. Montemerlo, "Fastslam: A factored solution to the simultaneous localization and mapping problem with unknown data association," in *Proc. AAAI Nat. Conf. Artif. Intell. (AAAI)*, Jul. 2003, pp. 593–598.
- [17] G. Grisetti, R. Kummerle, C. Stachniss, and W. Burgard, "A tutorial on graph-based SLAM," *IEEE Intell. Transp. Syst. Mag.*, vol. 2, no. 4, pp. 31–43, 2010. [Online]. Available: <https://ieeexplore.ieee.org/document/5681215/citations?tabFilter=patents#anchor-patent-citations>
- [18] V. Ila, J. M. Porta, and J. Andrade-Cetto, "Information-based compact pose SLAM," *IEEE Trans. Robot.*, vol. 26, no. 1, pp. 78–93, Feb. 2010.
- [19] G. E. Monahan, "State of the art—A survey of partially observable Markov decision processes: Theory, models, and algorithms," *Manage. Sci.*, vol. 28, no. 1, pp. 1–16, Jan. 1982.
- [20] L. Tai and M. Liu, "Mobile robots exploration through CNN-based reinforcement learning," *Robot. Biomimetics*, vol. 3, no. 1, p. 24, Dec. 2016.
- [21] S. Bai, F. Chen, and B. Englot, "Toward autonomous mapping and exploration for mobile robots through deep supervised learning," in *Proc. IEEE Int. Conf. Intell. Robots Syst. (IROS)*, Sep. 2017, pp. 2379–2384.
- [22] P. Mirowski *et al.*, "Learning to navigate in complex environments," in *Proc. Int. Conf. Learn. Represent. (ICLR)*, Toulon, France, Apr. 2017.
- [23] D. Pathak, P. Agrawal, A. A. Efros, and T. Darrell, "Curiosity-driven exploration by self-supervised prediction," in *Proc. IEEE Int. Conf. Mach. Learn. (ICML)*, Jul. 2017, pp. 16–17.
- [24] O. Zhelo, J. Zhang, L. Tai, M. Liu, and W. Burgard, "Curiosity-driven exploration for mapless navigation with deep reinforcement learning," 2018, *arXiv:1804.00456*. [Online]. Available: <https://arxiv.org/abs/1804.00456>

- [25] J. Yao, C. Lin, X. Xie, A. J. Wang, and C.-C. Hung, "Path planning for virtual human motion using improved A* star algorithm," in *Proc. IEEE Int. Conf. Inf. Technol., New Generat. (ITNG)*, Apr. 2010, pp. 1154–1158.
- [26] C. Rösmann, F. Hoffmann, and T. Bertram, "Kinodynamic trajectory optimization and control for car-like robots," in *Proc. IEEE Int. Conf. Intell. Robots Syst. (IROS)*, Sep. 2017, pp. 5681–5686.
- [27] E. Parisotto and R. Salakhutdinov, "Neural map: Structured memory for deep reinforcement learning," 2017, *arXiv:1702.08360*. [Online]. Available: <https://arxiv.org/abs/1702.08360>
- [28] Q. Zhang, D. Zhao, and D. Wang, "Event-based robust control for uncertain nonlinear systems using adaptive dynamic programming," *IEEE Trans. Neural Netw. Learn. Syst.*, vol. 29, no. 1, pp. 37–50, Jan. 2018.
- [29] Y. F. Chen, M. Liu, M. Everett, and J. P. How, "Decentralized non-communicating multiagent collision avoidance with deep reinforcement learning," in *Proc. IEEE Int. Conf. Robot. Autom. (ICRA)*, May/Jun. 2017, pp. 285–292.
- [30] D. Li, D. Zhao, Q. Zhang, and Y. Chen, "Reinforcement learning and deep learning based lateral control for autonomous driving," *IEEE Comput. Intell. Mag.*, vol. 14, no. 2, pp. 83–98, May 2019.
- [31] C. Chen, A. Seff, A. Kornhauser, and J. Xiao, "Deepdriving: Learning affordance for direct perception in autonomous driving," in *Proc. IEEE Int. Conf. Comput. Vis. (ICCV)*, Dec. 2015, pp. 2722–2730.
- [32] D. Zhao, Y. Chen, and L. Lv, "Deep reinforcement learning with visual attention for vehicle classification," *IEEE Trans. Cogn. Devel. Syst.*, vol. 9, no. 4, pp. 356–367, Dec. 2017.
- [33] Y. Chen, D. Zhao, L. Lv, and Q. Zhang, "Multi-task learning for dangerous object detection in autonomous driving," *Inf. Sci.*, vol. 432, pp. 559–571, Mar. 2018.
- [34] Z. Wang, T. Schaul, M. Hessel, H. Van Hasselt, M. Lanctot, and N. De Freitas, "Dueling network architectures for deep reinforcement learning," in *Proc. IEEE Int. Conf. Mach. Learn. (ICML)*, Jun. 2016, pp. 1995–2003.
- [35] E. B. Olson, "Real-time correlative scan matching," in *Proc. IEEE Int. Conf. Robot. Autom. (ICRA)*, Jun. 2009, pp. 4387–4393.
- [36] R. Kümmeler, G. Grisetti, H. Strasdat, K. Konolige, and W. Burgard, "G²o: A general framework for graph optimization," in *Proc. IEEE Int. Conf. Robot. Autom. (ICRA)*, May 2011, pp. 3607–3613.
- [37] B. Gerkey, R. T. Vaughan, and A. Howard, "The player/stage project: Tools for multi-robot and distributed sensor systems," in *Proc. IEEE Int. Conf. Adv. Robot. (ICAR)*, vol. 1, Jun./Jul. 2003, pp. 317–323.
- [38] F. Ramos and L. Ott, "Hilbert maps: Scalable continuous occupancy mapping with stochastic gradient descent," *Int. J. Robot. Res.*, vol. 35, no. 14, pp. 1717–1730, Jan. 2016.
- [39] T. Ergen and S. S. Kozat, "Efficient Online learning algorithms based on LSTM neural networks," *IEEE Trans. Neural Netw. Learn. Syst.*, vol. 29, no. 8, pp. 3772–3783, Aug. 2018.



Haoran Li received the B.S. degree in detection, guidance and control technology from Central South University, Changsha, China, in 2015. He is currently pursuing the Ph.D. degree in control theory and control engineering with the State Key Laboratory of Management and Control for Complex Systems, Institute of Automation, Chinese Academy of Sciences, Beijing, China.

His current research interests include deep reinforcement learning and autonomous driving.



Chichao Zhang received the B.S. degree in automation from Northeastern Electric Power University, Jilin, China, in 2012, the M.S. degree in control theory and control engineering from Northeast University, Shenyang, China, in 2014, and the Ph.D. degree in control theory and control engineering from the State Key Laboratory of Management and Control for Complex Systems, Institute of Automation, Chinese Academy of Sciences, Beijing, China, in 2017.

He is currently an Assistant Professor with the State Key Laboratory of Management and Control for Complex Systems, Institute of Automation, Chinese Academy of Sciences. His current research interests include reinforcement learning, game theory, and multi-agent systems.



Dongbin Zhao (M'06–SM'10) received the B.S., M.S., and Ph.D. degrees from the Harbin Institute of Technology, Harbin, China, in 1994, 1996, and 2000, respectively.

He was a Post-Doctoral Fellow with Tsinghua University, Beijing, China, from 2000 to 2002. He has been a Professor with the Institute of Automation, Chinese Academy of Sciences, Beijing, since 2002, and the University of Chinese Academy of Sciences, Beijing. From 2007 to 2008, he was a Visiting Scholar with The University of Arizona, Tucson, AZ, USA. He has published four books and over 80 international journal papers. His current research interests include the areas of deep reinforcement learning, computational intelligence, autonomous driving, game artificial intelligence, robotics, and smart grids.

Dr. Zhao was the Chair of the Beijing Chapter, Adaptive Dynamic Programming and Reinforcement Learning Technical Committee, from 2015 to 2016 and the Multimedia Subcommittee from 2015 to 2016 of the IEEE Computational Intelligence Society (CIS). He is the Chair of the Technical Activities Strategic Planning Sub-Committee. He is also a guest editor for renowned international journals. He is also involved in organizing many international conferences. He serves as an Associate Editor for the *IEEE TRANSACTIONS ON NEURAL NETWORKS AND LEARNING SYSTEMS*, *IEEE TRANSACTIONS ON CYBERNETICS*, and *IEEE Computational Intelligence Magazine*.